Chemical Physics Letters 644 (2016) 68–72

Contents lists available at ScienceDirect

Chemical Physics Letters

journal homepage: www.elsevier.com/locate/cplett

Formation of Ag nanoparticles on metastable β-Ag_2WO_4 microcrystals induced by electron irradiation

Roman Alvarez Roca [a,*], Pablo S. Lemos [a], Juan Andrés [b], Elson Longo [a,c]

[a] DQ-Universidade Federal de Sa˜o Carlos, P.O. Box 676, CEP, Sa˜o Carlos-SP 13565-905, Brazil
[b] Department of Analytical and Physical Chemistry, University Jaume I (UJI), Castelló 12071, Spain
[c] CDMF-Universidade Estadual Paulista, P.O. Box 355, Araraquara-SP 14801-907, Brazil

ARTICLE INFO

Article history:
Received 15 October 2015
In final form 27 November 2015
Available online 10 December 2015

ABSTRACT

In the present work, an easy precipitation method without presence of surfactants is applied to the synthesis of the hexagonal phase of metastable β-Ag_2WO_4 microcrystals at room temperature. In addition, we report for first time the *in situ* formation, growth, and subsequent reabsorption of Ag nanoparticles on the surface of this metastable phase, which was induced by electron beam irradiation under high *vacuum*.

1. Introduction

Addition of small amounts of noble metal nanoparticles (NPs), such as Ag, to semiconductors is an effective procedure for enhancing the visible light absorption and photocatalytic activity, which is related to the surface plasmon resonance of noble metal NPs and lead to the separation of electron–hole pairs [1–4]. In these modified semiconductors, electron–hole separation rates at the semiconductor surface are enhanced by surface plasmon resonance from the noble metal nanostructures. The possibility of building new nanostructures by combining noble metals and semiconductors opens a wide spectrum of desirable synergistic and complementary effects. The combination of these two dissimilar materials in a controlled way is an interesting challenge. The modified materials by using of Ag NPs are of particular interest because of their outstanding photocatalytic performances and their wide range of applications in solar cells, bactericide, chemical sensing, to name just a few examples.

Recently, our group reported, for the first time, the *in situ* nucleation and growth of Ag NPs on an α-Ag_2WO_4 surface driven by an accelerated electron beam under high *vacuum* (from an electronic microscope) [5–9]. In other Ag based materials, such as β-Ag_2MoO_4 [10,11] and Ag_3PO_4 [12], this phenomenon, as well as their applications as photocatalyst, sensor and bactericide, had also been reported and analyzed [6,7,10–15]. Several experimental techniques, combined with first-principles modeling based on density functional theory, were employed for materials characterization, and a mechanism for the Ag nucleation and growth process from the nano- to micro-scale has been proposed [5–12]. In recent years, different research groups have also reported interest in these materials due to their attractive properties and their widespread applications in many fields of nanotechnology [16–27].

Silver tungstate, Ag_2WO_4, is known for its various applications such as catalytic and photocatalytic activity [16–18,28,29], sensing [13], antibacterial activity [6,30] and optical and photoluminescent properties [7,14,15,19,31,32]. Ag_2WO_4 exist as three polymorphs [33]: an orthorhombic phase, α-Ag_2WO_4, which is the most thermodynamically stable phase and two metastable phases identified as β- and γ-Ag_2WO_4 with hexagonal and cubic spinel structures, respectively. The study of metastable phases has been elusive due to their propensity to convert to the more stable α-phase. Various methods to obtain different Ag_2WO_4 metastable phases have been reported [14,20,28,33–35]. In one such method, metastable β-Ag_2WO_4 was successfully prepared by precipitation using a surfactant-assisted route, in which the surfactant action prevented β- to α-phase transformation [28,34,35]. Other surfactant free routes such as precipitation at pH = 4 afford metastable β-Ag_2WO_4 with a small amount of the α-phase [14], and the synthesis of pure β-Ag_2WO_4 at low temperature [20] have also been reported. The β-Ag_2WO_4 phase was obtained by a surfactant-assisted precipitation method in the presence of polymethacrylic acid (PMAA) [28], polyvinylpyrrolidone (PVP) [34] or acrylamide (AM) [35] which prevents the phase transformation from the β- (metastable) to α-phase (stable). Similar synthetic conditions had been used in several studies, but in the final steps of the synthetic route various form of excitation energy were used, such as mechanical-thermal stimulation by microwave, conventional ovens or sonication [5,32,36], and the more stable α-phase was obtained as the final

* Corresponding author.
E-mail address: cortes116@yahoo.es (R. Alvarez Roca).

http://dx.doi.org/10.1016/j.cplett.2015.11.048
0009-2614/

product, showing that these perturbations, even when relatively small, induce the transition from the metastable toward the more stable phase.

One of the Holy Grails of modern chemistry is the synthesis and characterization of inorganic thermodynamically unstable or metastable materials that can have important properties when compared to those of their stable phase analogs. However, the synthesis of metastable phases of inorganic compounds is challenging but rewarding due to preferential transformation to the stable phase. In this communication, we synthesized metastable β-Ag_2WO_4 microcrystals using an easy precipitation method, and report, for the first time, the *in situ* formation and subsequent growth of Ag NPs on microcrystal surface of this metastable phase under electron beam irradiation. The understanding of this phenomenon will allow for an in-depth exploitation of the properties of Ag NPs on semiconductor surfaces.

2. Experimental

β-Ag_2WO_4 microcrystals were synthesized using a precipitation method as follows: 1 mmol of sodium tungstate (VI) dihydrate ($Na_2WO_4{\cdot}2H_2O$; 99.5% purity, Sigma–Aldrich) and 2 mmol of silver nitrate ($AgNO_3$; 99.8% purity, Sigma–Aldrich) were separately dissolved in 50 mL of deionized water and kept at pH 7–8. In the sequence, the solution with WO_4^{2-} ions was transferred to a 250 mL glass beaker with continuous stirring and then the second solution containing the Ag^+ ions was added to the glass beaker. An initial yellow suspension was formed and maintained at 25 °C with continued stirring for 20 min. The resulting white precipitate that formed was washed several times with deionized water and acetone to remove any remaining ions. Finally, the powdered precipitate was collected and dried at room temperature for 24 h.

The crystal symmetry of β-Ag_2WO_4 samples was characterized by powder X-ray diffraction (XRD) using a D/Max-2500PC diffractometer (Rigaku, Japan) with Cu-Kα radiation (λ = 1.5406 Å) in a 2θ range of 10° to 70° and a scanning velocity of 2°/min. The shapes and sizes of the β-Ag_2WO_4 particles, with and without Ag, nanoparticles were studied using an Inspect F50 field-emission scanning electron microscope (FE-SEM, FEI Company, Hillsboro, OR) with an operating range of 5–20 kV. Transmission electron microscopy analysis, TEM, was performed using a JEM 2100F TEM/STEM microscope operating at 200 kV. Chemical analyses of the sample were performed by Energy Dispersive X-Ray Spectroscopy (EDS) using an EDS Thermo-Noran equipped with a Si detector attached to JEM 2100F.

3. Results and discussion

The corresponding XRD pattern of the Ag_2WO_4 powders is shown in Figure 1a. The diffraction peaks observed were matched to the standard XRD data of hexagonal-phase Ag_2WO_4 (JCPDS file, no: 33-1195) with the space group P63. In contrast to previous studies, the conditions used in our work allowed the synthesis of the metastable β-phase without presence of any surfactant. It is important to note that small and subtle changes (for example pH [14], reactant's concentration [20,33], *etc.*) of the experimental conditions along the synthetic procedure are capable to modify the synthesis of both α- and β-phases.

The FE-SEM image shown in Figure 2 illustrates that the β-Ag_2WO_4 microparticles have a rod-like elongated shape with a polydisperse size distribution for both their length and width. A comparative analysis of the images reveals that this synthetic method produces β-Ag_2WO_4 crystals with larger sizes than the α-Ag_2WO_4 crystals reported previously [32].

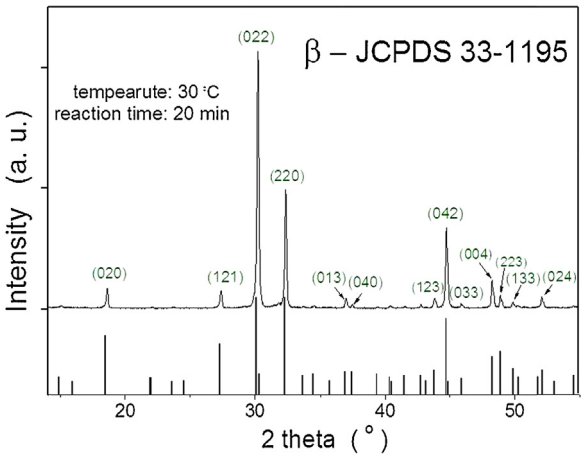

Figure 1. Powder XRD patterns of β-Ag_2WO_4 synthesized (continue line) with the Miller Index of the most intense peaks. The vertical lines indicate the position and relative intensity of the respective JCPDS card.

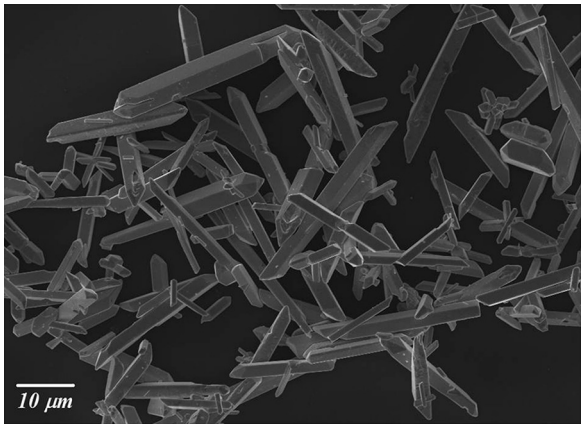

Figure 2. FE-SEM micrograph of the β-Ag_2WO_4 metastable phase.

The growth process of Ag NPs on the β-Ag_2WO_4 surface by electron irradiation is shown in the TEM micrographs in Figure 3. These metallic Ag NPs were very small and well dispersed on the surface of the β-Ag_2WO_4 and can serve as excellent acceptors to trap for electrons and they are capable of storing electrons. Hence, from a theoretical perspective, these electrons induced in the conduction band of β-Ag_2WO_4 could be quickly transferred to the Ag NPs instead of remaining in the β-Ag_2WO_4 lattice, which further facilitated charge separation. Subsequently, holes in the valence band of β-Ag_2WO_4 could act as oxidant centers, while the accumulated electrons on Ag NPs and the conduction band of β-Ag_2WO_4 could act as reduction centers. These effects modify their electronic properties and they can change their photocatalytic activity. This argument in line with recent experimental work of Chen and Xu [20] in which both α- and β-Ag_2WO_4 are tested for the photocatalytic degradation of phenol and azo-dye X3B in aqueous solutions, showing that β-Ag_2WO_4 was more photoactive, but less stable than α-Ag_2WO_4.

A view of the particle surface at initial time, which is assumed in the irradiation beginning, is shown in Figure 3a. The β-Ag_2WO_4 surface appeared clean and smooth while after exposure to electron irradiation for a time period, the growth of the Ag NPs on the surface of β-Ag_2WO_4 can be observed, as shown in Figure 3b and c. The typical morphologies of the Ag NPs are seen to be filaments and nearly spherical (highlighted with black arrows). The particles with nearly spherical format are less in number and slightly larger than the filament format. Finally, Figure 3d shows that after a longer exposure

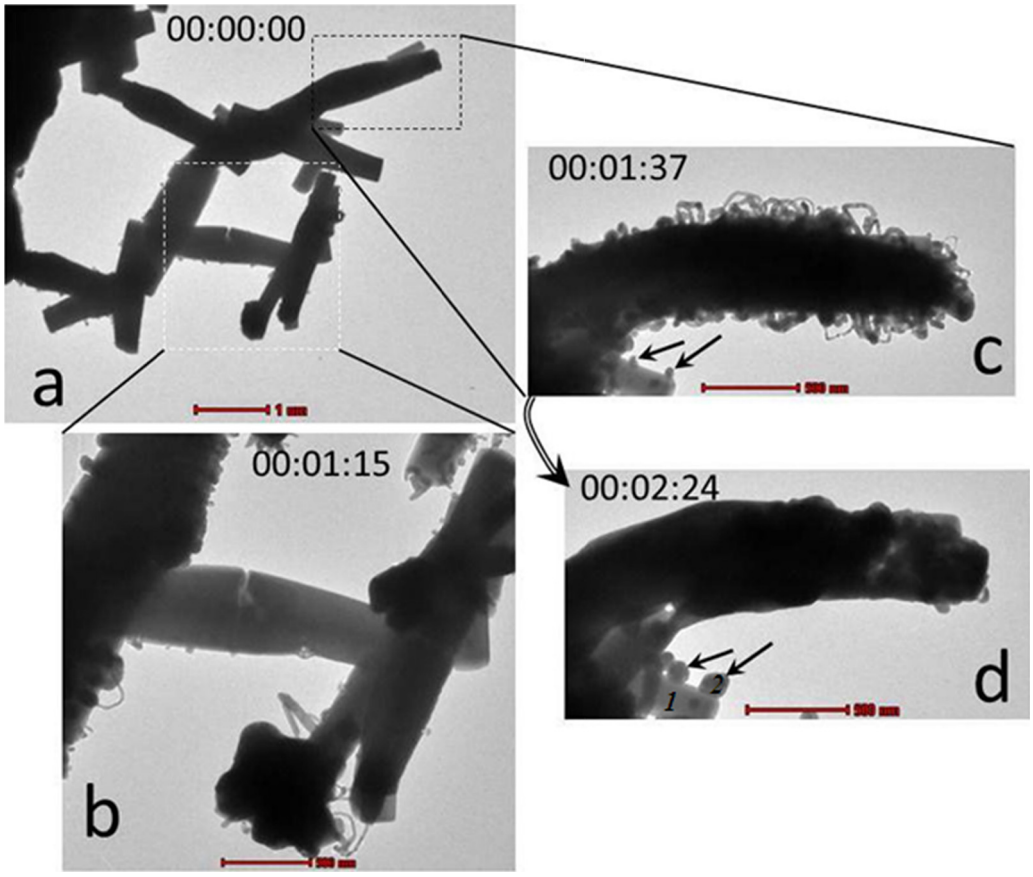

Figure 3. TEM micrograph showing the Ag NP growth on the β-Ag_2WO_4 surface. (a) Low magnification of the clean surface, (b, c) high magnification showing Ag NP growth on the microcrystals surface, and (d) reabsorption of Ag NPs. An EDX spectrum was collected at each point in the image. For more details see in text (Scale bar is 1 μm in (a) and 500 nm in (b–d)).

(2–3 min) to electron irradiation, the Ag NPs with the filament morphology were reabsorbed. Interestingly, some Ag NPs, which had a nearly spherical morphology, remained and, in contrast, these Ag NPs continued growing while the other was absorbed (see the black arrows in this Figure).

Energy dispersive spectroscopy (EDS) confirmed that Ag NPs grew on the β-Ag_2WO_4 surface, as is depicted in Figure 4, in which the nominal atomic percent of Ag and W in each region is listed. Although the events observed (nucleation, growth and complete reabsorption of Ag NPs) were dependent on the irradiation conditions, the entire process took place in only a few minutes and it was faster than the similar processes observed for α-Ag_2WO_4. A study in α-Ag_2WO_4 with a similar synthetic method showed that changes in the synthesis parameters led to changes in the samples organization (from point of view of the order, symmetry, cluster distortion, *etc.*) and in the most organized samples, a higher nucleation rate of Ag NPs, as well as a higher absorption was observed [32]. In the present study, if a higher organization in the β-Ag_2WO_4 hexagonal structure is assumed, in comparison with the α-Ag_2WO_4 orthorhombic structure, then it is possible to explain the faster nucleation and absorption of Ag NPs in β-Ag_2WO_4.

The growth and reabsorption processes are presented in Figure 5 by scanning electron microscopy (FE-SEM) images. In the micrograph of Figure 5a, the Ag NPs grew on the surface after a certain period of irradiation. At this instant, the irradiation power was increased and maintained for 100 s. After this time, the reabsorption of almost all the Ag NPs was observed, while some few isolated Ag NPs remained and increased in size (see Figure 5b). This further growth could be a result of the accumulation of the Ag NPs at singular points on the surface. A located Ag NPs accumulation at the end of the microcrystal, which resulted in the growth of a thicker filament that grew further, was observed for α-Ag_2WO_4 [8].

A revision of literature renders that under the electron beam irradiation, formation of metal nanoparticles, such as Cu [37], Au [38], In [39], Bi [40], Co [41], and Os [42] The real *in situ* observations of these novel phenomena can only be observed at atomic scale. We point out that electron beams from FE-SEM provide a new type of electron-matter interactions in which energetic electrons with the sample may cause significant perturbations in the system under observation. In the above context, a deep understanding of the interactions between the electrons and the irradiated material is necessary to interpret the processes occurring and to extract mechanistic information. José-Yacamán et al. [43] have been studied the surface diffusion and coalescence of mobile metal nanoparticles, and they highlighted the characteristic of liquid-like behavior of the coalescence process [44]. Buffat [45] have been analyzed the dynamical behavior of nanocrystals in transmission electron microscopy. But, it is important to note that the realistic temperature on the specimen inside a FE-SEM is below the melting point; then the heating effect caused by the phonons from the electron beam on the growth of metal nanoparticles can be discarded [46].

Future investigations will be conducted to confirm the true potential of the systems studied here and offer new possibilities for creating complex functional materials that can be optimized for a large number of biological, catalytic, photoluminescence and other emerging applications. In addition, a detailed investigation is necessary to provide further insight into the effects of the superficial irregularities; as corners (at the end of elongate particles), kinks, islands and others surface singularities. These irregularities may act as 'traps' for Ag NPs accumulation, and thereby, suppress

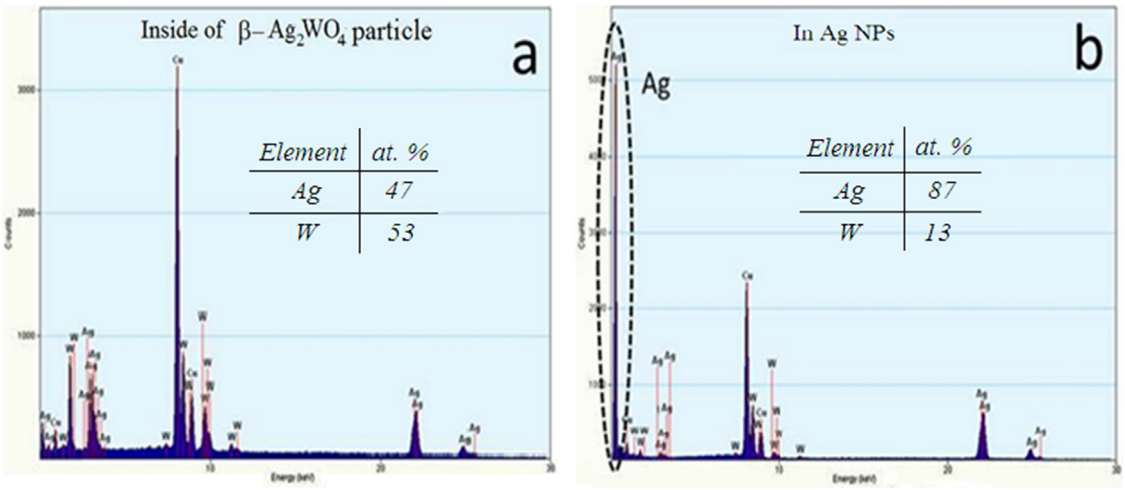

Figure 4. EDS performed in different regions of β-Ag_2WO_4 microcrystals. The spectrum was collected at each point identified in Figure 3(d): point 1 and 2 are inside of β-Ag_2WO_4 and inside of Ag NPs, respectively.

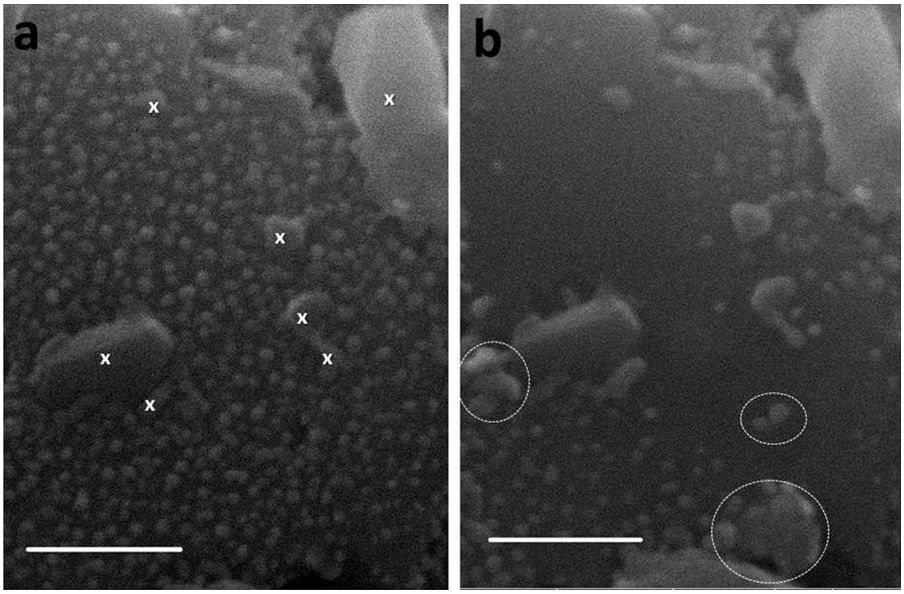

Figure 5. FE-SEM micrographs of β-Ag_2WO_4, showing growth and reabsorption of Ag NPs, (a) before, and (b) after electron irradiation for 100 s. The Ag NPs ranged in size from 12 to 16 nm. In (a) non Ag particles are indicated with X, and in (b) dashed line circles are Ag NPs with excessive growth (Scale bar is 200 nm).

the reabsorption and promote the growth of thicker and isolated Ag NPs.

To complement this experimental work, a theoretical study is in progress by our research group in order to: (i) study in detail the structural and electronic aspects of β-Ag_2WO_4 using first-principles electronic structure theory calculations. In particular, we have calculated by full optimization the lattice parameters, and the corresponding values: $a = 11.0847$ Å and $c = 7.7099$ Å (cell volume = 820.417 $Å^3$) were obtained. Two kinds of clusters coordination were founded both W (W1 and W2) and Ag (Ag1 and Ag2) atoms. W1 atoms are coordinate to four O atoms, which form distorted tetrahedral [WO_4] clusters, while the W2 atoms are at the center of distorted trigonal bipyramidal [WO_5] clusters. Ag1 atoms are coordinated to six O atoms, which form distorted octahedral [AgO_6] clusters, while the Ag2 atoms belong to distorted trigonal bipyramidal [AgO_5] clusters [47]. (ii) Confirm the proposed structure of the β-Ag_2WO_4 phase and how it can be transformed to the stable orthorhombic α-Ag_2WO_4 phase, and (iii) elucidate the effects of the metastable character of the β-Ag_2WO_4 phase on the nucleation and growth of Ag NPs.

4. Conclusions

In this work, we report the synthesis of metastable phase β-Ag_2WO_4 *via* a simple precipitation method without presence of surfactants and, for first time, the *in situ* formation, growth and subsequent reabsorption of Ag NPs on the surface of the β-Ag_2WO_4 metastable phase. X-ray diffraction, transmission and scanning electronic microscopies, and energy dispersive spectroscopy have been used for the characterization of the microcrystals and the Ag NPs obtained. β-Ag_2WO_4 metastable phase is a complex functional material, and the presence of Ag NPs on their surfaces are expected to have practical applications in photocatalysis, microelectrodes, or sensors.

Acknowledgments

This work was financially supported by the following Brazilian research funding institutions: Fundação de Amparo à Pesquisa do Estado de São Paulo (FAPESP; 2012/14004-5 and 2013/07296-2), Conselho Nacional de Desenvolvimento Científico e Tecnológico

(CNPq; 479644/2012-8, 350711/2012-7, 304531/2013-8 and 151136/2013-0). Coordenação de Aperfeiçoamento de Pessoal de Nível Superior (CAPES). J. A. acknowledges also the financial support of the Spanish research funding projects: *PrometeoII*/2014/022 and ACOMP/2014/270 projects (Generalitat-Valenciana), Ministerio de Economia y Competitividad (CTQ2012-36253-C03-02) and Programa de Cooperacioón Cientifiíca con Iberoamerica (Brasil), Ministerio de Educacioín (PHB2009-0065-PC).

References

[1] S. Linic, P. Christopher, D.B. Ingram, Nat. Mater. 10 (2011) 911.
[2] C. Yu, L. Wei, X. Li, J. Chen, Q. Fan, J.C. Yu, Mater. Sci. Eng. B 178 (2013) 344.
[3] Y.J. Luo, X.M. Liu, X.H. Tang, Y. Luo, Q.Y. Zeng, X.L. Deng, S.L. Ding, Y.Q. Sun, J. Mater. Chem. A 2 (2014) 14927.
[4] J.B. Priebe, J. Radnik, A.J.J. Lennox, M.M. Pohl, M. Karnahl, D. Hollmann, K. Grabow, U. Bentrup, H. Junge, M. Beller, A. Brückner, ACS Catal. 5 (2015) 2137.
[5] E. Longo, L.S. Cavalcante, D.P. Volanti, A.F. Gouveia, V.M. Longo, J.A. Varela, M.O. Orlandi, J. Andres, Sci. Rep. 3 (2013) 1676.
[6] V.M. Longo, C.C. De Fogg, M.M. Ferrer, A.F. Gouveia, R.S. André, W. Avansi, C.E. Vergani, A.L. Machado, J. Andrés, L.S. Cavalcante, A.C. Hernandes, E. Longo, J. Phys. Chem. A 118 (2014) 5769.
[7] E. Longo, D.P. Volanti, V.M. Longo, L. Gracia, I.C. Nogueira, M.A.P. Almeida, A.N. Pinheiro, M.M. Ferrer, L.S. Cavalcante, J. Andres, J. Phys. Chem. C 118 (2014) 1229.
[8] J. Andrés, L. Gracia, P. Gonzalez-Navarrete, V.M. Longo, W. Avansi Jr., D.P. Volanti, M.M. Ferrer, P.S. Lemos, F.A.L. Porta, A.C. Hernandes, E. Longo, Sci. Rep. 5 (2014) 5391.
[9] W. da Silva Pereira, J. Andrés, L. Gracia, M.A. San-Miguel, E.Z. da Silva, E. Longo, V.M. Longo, Phys. Chem. Chem. Phys. 17 (2015) 5352.
[10] J. Andrés, M.M. Ferrer, L. Gracia, A. Beltran, V.M. Longo, G.H. Cruvinel, R.L. Tranquilin, E. Longo, Part. Part. Syst. Charact. 32 (2015) 646.
[11] M.T. Fabbro, C. Saliby, L.R. Rios, F.A. La Porta, L. Gracia, M.S. Li, J. Andrés, L.P.S. Santos, E. Longo, Sci. Technol. Adv. Mater. 16 (2015) 065002.
[12] G. Botelho, J.C. Sczancoski, J. Andres, L. Gracia, E. Longo, J. Phys. Chem. C 119 (2015) 6293.
[13] L.F. da Silva, A.C. Catto, W. Avansi, L.S. Cavalcante, J. Andres, K. Aguir, V.R. Mastelaro, E. Longo, Nanoscale 6 (2014) 4058.
[14] Y.V.B. De Santana, J.E.C. Gomes, L. Matos, G.H. Cruvinel, A. Perrin, C. Perrin, J. Andrès, J.A. Varela, E. Longo, Nanomater. Nanotechnol. 4 (2014) 22.
[15] R.A. Roca, J.C. Sczancoski, I.C. Nogueira, M.T. Fabbro, H.C. Alves, L. Gracia, L.P.S. Santos, C.P. de Sousa, J. Andrés, G.E. Luz, E. Longo, L.S. Cavalcante, Catal. Sci. Technol. 5 (2015) 4091.
[16] R. Zhang, H. Cui, X. Yang, H. Tang, H. Liu, Y. Li, Micro Nano Lett. 7 (2012) 1285.
[17] M. Vafaeezadeh, M.M. Hashemi, RSC Adv. 5 (2015) 31298.
[18] Z. Lin, J. Li, Z. Zheng, J. Yan, P. Liu, C. Wang, G. Yang, ACS Nano 9 (2015) 7256.
[19] A. Sreedevi, K.P. Priyanka, S.R. Mary, E.M. Mohammed, T. Varghese, Adv. Sci. Eng. Med. 7 (2015) 498.
[20] H. Chen, Y. Xu, Appl. Surf. Sci. 319 (2014) 319.
[21] D.P. Dutta, A. Singh, A. Ballal, A.K. Tyagi, Eur. J. Inorg. Chem. 2014 (2014) 5724.
[22] L. Pan, L. Li, Y.H. Chen, J. Sol-Gel Sci. Technol. 66 (2013) 330.
[23] C. Janáky, K. Rajeshwar, N.R.D. Tacconi, W. Chanmanee, M.N. Huda, Catal. Today 199 (2013) 53.
[24] C.H. Bernard, W.Y. Fan, Cryst. Growth Des. 15 (2015) 3032.
[25] Z.Y. Bao, D.Y. Lei, J. Dai, Y. Wua, Appl. Surf. Sci. 287 (2013) 404.
[26] M. Ramezani, S.M. Pourmortazavi, M. Sadeghpur, A. Yazdani, I. Kohsari, J. Mater. Sci.: Mater. Electron. 26 (2015) 3861.
[27] D. Xu, B. Cheng, J. Zhang, W. Wang, J. Yu, W. Ho, J. Mater. Chem. A (2015), http://dx.doi.org/10.1039/c0xx00000x.
[28] X. Wang, C. Fu, P. Wang, H. Yu, J. Yu, Nanotechnology 24 (2013) 165602.
[29] J. Tang, J. Ye, J. Mater. Chem. 15 (2005) 4246.
[30] X. Sang, P. Wang, L. Ai, Y. Li, J. Bu, Adv. Mater. Res. 284–286 (2011) 1321.
[31] S.H. Yu, B. Liu, M. Mo, J.H. Huang, X.M. Liu, Y.T. Qian, Adv. Funct. Mater. 13 (2003) 639.
[32] L.S. Cavalcante, M.A.P. Almeida, W. Avansi, R.L. Tranquilin, E. Longo, N.C. Batista, V.R. Mastelaro, L.M. Siu, Inorg. Chem. 51 (2012) 10675.
[33] A.J. Van den Berg, C.A.H. Juffermans, J. Appl. Cryst. 15 (1982) 114.
[34] J. Li, C. Yu, C. Zheng, A. Etogo, Y. Xie, Y. Zhong, Y. Hu, Mater. Res. Bull. 61 (2014) 315.
[35] X.Y. Zhang, J.D. Wang, J.K. Liu, X.H. Yang, Y. Lu, CrystEngComm 17 (2015) 1129.
[36] H. Muller-Buschbaum, Z. Anorg. Allg. Chem. 630 (2004) 2125.
[37] P.I. Wang, Y.P. Zhao, G.C. Wang, T.M. Lu, Nanotechnology 15 (2004) 218.
[38] J.U. Kim, S.H. Cha, K. Shin, J.Y. Jho, J.C. Lee, J. Am. Chem. Soc. 127 (2005) 9962.
[39] D. Golberg, M. Mitome, L.W. Yin, Y. Bando, Chem. Phys. Lett. 416 (2005) 321.
[40] S.H. Kim, Y.S. Choi, K. Kang, S.I. Yang, J. Alloys Compd. 427 (2007) 330.
[41] T. Gnanavel, G. Möbus, J. Phys.: Conf. Ser. 371 (2012) 012047.
[42] A. Pitto-Barry, L.M.A. Perdigao, M. Walker, J. Lawrence, G. Costantini, P.J. Sadler, N.P.E. Barry, Dalton Trans. (2015), http://dx.doi.org/10.1039/C5DT03205A.
[43] M. José-Yacamán, C. Gutierrez-Wing, M. Miki, D.Q. Yang, K.N. Piyakis, E. Sacher, J. Phys. Chem. B 109 (2005) 9703.
[44] G. Casillas, A. Ponce, J.J. Velazquez-Salazar, M. Jose-Yacamán, Nanoscale 5 (2013) 6333.
[45] P.A. Buffat, Philos. Trans. R. Soc. Lond. A 361 (2003) 291.
[46] D.B. Williams, C.B. Carter, Transmission Electron Microscopy: A Textbook for Materials Science, 2nd edn., Springer, New York; London, 2009, lxii, 760 p., I1-15.
[47] P.S. Lemos, A. Altomare, A.F. Gouveia, I.C. Nogueira, L. Gracia, R. Llusar, J. Andrés, E. Longo, L.S. Cavalcante, Dalton Trans., 2015 (to be published).